

Relations between transient charge transport and the glass-transition temperature in amorphous chalcogenides

Hiroyoshi Naito

Department of Physics and Electronics, University of Osaka Prefecture, Gakuencho, Sakai, Osaka 593, Japan

Yoshihiko Kanemitsu

Institute of Physics, University of Tsukuba, Tsukuba, Ibaraki 305, Japan

(Received 14 July 1993; revised manuscript received 1 December 1993)

Relations between transient charge transport and the glass-transition temperature, T_g , have been investigated in amorphous Se-based chalcogenides. The phenomenological relationship between the extrapolated zero-field drift-mobility activation energy, E_0 , and the glass-transition temperature, T_g , is found to be $E_0 = 1.2 \times 10^{-3} T_g$ in these materials, where the units of E_0 and T_g are eV and K, respectively. This relation can be understood by considering that the transient transport of photoinjected carriers is controlled by multiple trapping in an exponential-tail state, whose width is solely determined by T_g .

I. INTRODUCTION

Transient charge transport in amorphous photoconductors has been extensively studied from the theoretical as well as experimental points of view.^{1,2} This stems from their practical importance in electrophotography and from their importance for the understanding of amorphous states.

Most of the amorphous photoconductors are glassy materials, and thus exhibit glass transition. The glass-transition temperature T_g is one of the most important thermodynamical parameters for the characterization of glassy states. For example, physical quantities, such as the melting temperature,³ the magnitude of photodarkening,⁴ and the width of the Urbach tail^{5,6} of the materials can be related to T_g . It is therefore important to explore how the glass transition relates to the transient charge transport processes in the amorphous photoconductors.

In the present study, we report on the phenomenological relationship between transient transport properties and T_g in typical amorphous photoconductors, amorphous Se-based chalcogenides. Our experimental findings are examined in light of theories concerning transient transport and electronic structures in the glasses.

II. TRANSIENT CHARGE TRANSPORT OF AMORPHOUS SEMICONDUCTORS

A variety of electronic and optical properties of a -Se and a -As₂Se₃ have been reported,² because these two materials are regarded as prototypical amorphous chalcogenides. Transient charge transport of these materials has been extensively studied with the time-of-flight (TOF) experimental technique in a sample with a sandwich-electrode configuration.² Transient pulse shapes of a -Se and a -As₂Se₃ in the TOF experiment exhibit anomalous transit dispersion (the anomalous dispersion in a -Se is observed only in the temperature range below 180 K).^{7,8}

Tiedje and Rose⁹ and Orenstein and Kastner¹⁰ have successfully explained these results on the basis of the multiple-trapping (MT) model and have employed the concept of a thermalization energy E_{th} , separating shallow from deep trapping centers, defined as $E_{th} = kT \ln(\nu t)$, where t is the elapsed time after the creation of the excess carriers, and ν is the attempt-to-escape frequency of the centers. For an assumed exponential energy dependence of the tail-state distribution,

$$g(E) = g_0 \exp(-E/kT_0), \quad (1)$$

where T_0 is the width of the distribution in a temperature unit, an expression for the drift mobility, μ_d , can be derived as

$$\mu_d = \nu \left[\frac{\nu}{1-\alpha} \right]^{-1/\alpha} \mu_0^{1/\alpha} \left[\frac{F}{L} \right]^{1/\alpha-1}, \quad (2)$$

where $\alpha = T/T_0$, μ_0 is the microscopic mobility of free holes at the mobility edge of the valence band, L is the thickness of the sample, and F is the applied electric field. In Fig. 1(a) we show the temperature dependence of the drift mobility at various electric fields calculated from Eq. (2) as closed symbols with the appropriate values for a -As₂Se₃ ($\nu = 10^{12}$ Hz, $T_0 = 500$ K, $\mu_0 = 0.1$ cm²/V s, $L = 1$ μ m).^{11,12} It can be seen from this figure that the drift mobilities exhibit thermally activated behavior, which is in excellent agreement with experimental results in a vast class of amorphous solids.^{1,2} Figure 1(b) shows the calculated drift-mobility activation energy plotted against $F^{1/2}$ as closed circles using the same values as described above.

It has been reported that the temperature and electric-field dependences of the hole drift mobilities in a -Se and a -As₂Se₃ obey Gill's phenomenological expression^{2,13,14} as well, which is

$$\mu_d = \mu'_0 \exp[-(E_0 - \beta F^{1/2})/kT_{eff}], \quad (3)$$

where $1/T_{\text{eff}} = 1/T - 1/T'_0$, μ'_0 is the mobility at $T = T'_0$, β is a constant coefficient, T'_0 is the temperature at which extrapolated temperature dependences at different fields intersect, and E_0 is the zero-field activation energy. This empirical expression was originally used for the analysis of transient transport in amorphous organic polymers such as poly-N-vinyl carbazole.² The electric-field dependence of the mobilities expressed in Eq. (3) can be most easily explained by applying the Poole-Frenkel mechanism to a trap-controlled mobility model. This model predicts the lowering of a Coulomb potential well in the direction of the applied field, so that the effective trap depth, and hence the activation energy, decreases as the square root of the field. If this is the case, β in Eq. (3) is the Poole-Frenkel coefficient and is given by

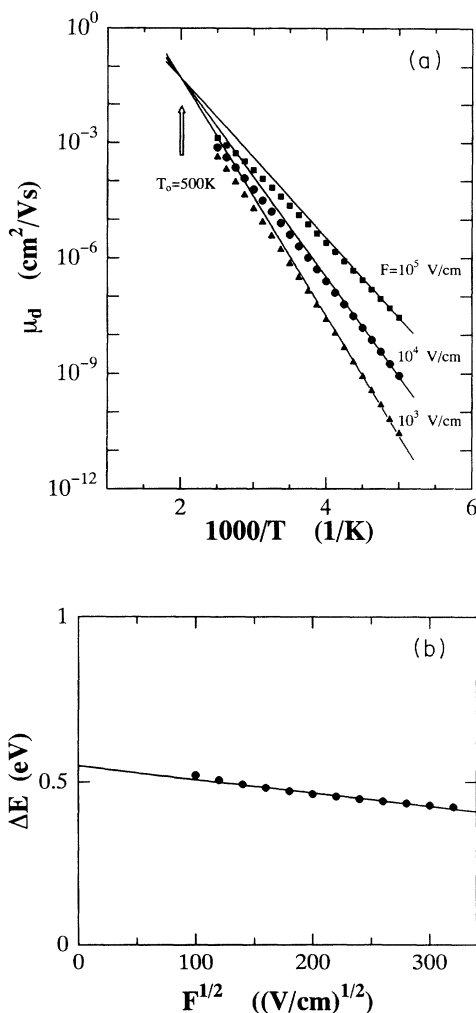


FIG. 1. (a) Temperature dependence of the drift mobility at different electric fields calculated from Eq. (2) with $\nu = 10^{12}$ Hz, $T_0 = 500$ K, $\mu_0 = 0.1$ cm²/V s, and $L = 1$ μ m. The solid lines represent the best-fitted Gill's expression. (b) Electric-field dependence of the drift-mobility activation energy calculated from Eq. (2) with $\nu = 10^{12}$ Hz, $T_0 = 500$ K, $\mu_0 = 0.1$ cm²/V s, and $L = 1$ μ m. The solid line represents the electric-field dependence of the activation energy of the best-fitted Gill's expression.

$(q^3/\pi\epsilon\epsilon_0)^{1/2}$, where q is the electronic charge and $\epsilon\epsilon_0$ is the dielectric constant of the material. This simple interpretation can be found in the literature.¹³⁻¹⁵ However, the experimental β coefficients do not always correspond to the Poole-Frenkel coefficient for amorphous organic polymers as well as amorphous chalcogenides.^{13,14,16}

It should be noted that Gill's phenomenological expression can be fitted to the drift-mobility data calculated from the MT expression Eq. (2). Best-fitted results are shown in Figs. 1(a) and 1(b) as solid lines. This is the reason why experimental results for *a*-Se and *a*-As₂Se₃ can be analyzed by Gill's expression as well as the MT expression.

III. RESULTS AND DISCUSSION

We focus ourselves to the results of Se-based chalcogenides in the present study, because the chalcogenides are typical photoreceptor materials and because much information concerning both T_g and transient transport properties is available for the glasses. Since in most Se-based glasses the drift mobilities of holes are much larger than those of electrons and exhibit activated temperature dependence,¹ we examine a relation between the zero-field drift-mobility activation energy for holes and T_g , and that between the microscopic mobility and T_g . Since the activation energy ΔE is electric field dependent in these materials, we take the extrapolated zero-field values E_0 determined in the plots of ΔE vs \sqrt{F} .

Figure 2 shows a plot of E_0 versus T_g for various Se-based chalcogenide thin films. Some of the data are taken from literature,^{13,14,17-21} and the rest of the data are our experimental data for the thin-film samples of amorphous chalcogenide deposited on the substrate held at T_g by

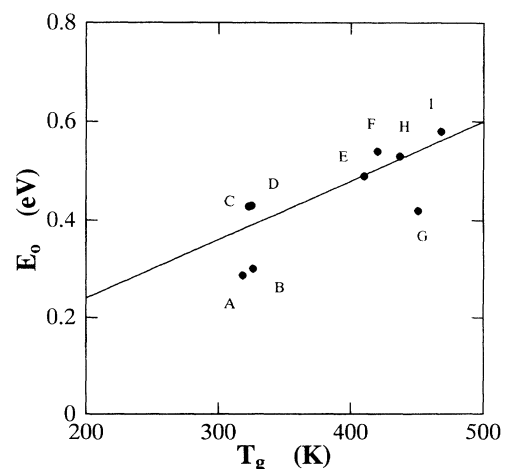


FIG. 2. A plot of the zero-field drift-mobility activation energy E_0 vs the glass-transition temperature T_g for various Se-based chalcogenides. Data for (A) *a*-Se (Ref. 13); (B) *a*-(5 at. % As): Se (Ref. 14); (C) *a*-(3.2 at. % Te): Se (Ref. 17); (D) *a*-(5 at. % Te): Se (Ref. 17); (E) *a*-(8 at. % Te):As₂Se₃; (F) *a*-(4 at. % Te):As₂Se₃; (G) *a*-GeSe₄ (Ref. 18); (H) *a*-AsSe (Ref. 19); and (I) *a*-As₂Se₃ (Ref. 20). The solid line $E_0 = 1.2 \times 10^{-3} T_g$ is the best-fitted line to the data.

vacuum evaporation. It is clearly seen that E_0 in units of eV is proportional to T_g in units of K; the solid line in the figure is the best-fitted line to the data, and is given by

$$E_0 = 1.2 \times 10^{-3} T_g . \quad (4)$$

We will show that Eq. (4) can be explained by a combination of the MT (Refs. 9 and 10) and the quantum-well (QW) model,⁶ implying that the MT of photoinjected carriers in valence band into an exponential-tail state controls transient charge transport, and the width of the tail state is solely determined by T_g in the materials.

Since the extrapolated zero-field values E_0 have been determined from the plots of ΔE vs \sqrt{F} , it is important to relate Gill's expression to the MT expression. In the framework of the MT model, it is easy to show that drift mobilities can be expressed as

$$\mu_d = \frac{\mu_0}{2} \exp(-\Delta E/kT_{\text{eff}}) , \quad (5)$$

where $1/T_{\text{eff}} = 1/T - 1/T_0$, and

$$\Delta E = kT_0 \ln \left[2\nu \frac{L}{\mu_0 F} \right] . \quad (6)$$

It is evident from Eqs. (3) and (5) that the temperature dependence of the MT expression is identical to that of Gill's expression, because $1 - \alpha$ exhibits rather weak temperature dependence in comparison with $\exp(-\Delta E/kT)$ and can be approximated to 0.5, the value at $T = T_0/2$, in the temperature range of interest here as manifested from Fig. 1(a). This approximation is due to the fact that the drift-mobility activation energies are determined in the temperature range $0.3T_0 < T < 0.7T_0$ in almost all experiments.^{1,2,13,14,16-20} The electric-field dependence of the drift-mobility activation energy due to the MT is almost identical to that due to Gill's expression, as shown in Fig. 1(b) in the electric-field range from 10^4 to 10^5 V/cm, where E_0 and β values are determined in most cases.^{1,2,13,14,16-20} The electric-field dependence of the activation energy, $E_0 - \beta F^{1/2}$, in Gill's expression can thereby be fitted to Eq. (6). With a least-squares method in the electric-field range from F_1 to F_2 , E_0 and β can be determined as

$$E_0 = kT_0 \ln \left[2\nu \frac{L}{\mu_0 P(F_1, F_2)} \right] \quad (7)$$

and

$$\beta = kT_0 Q(F_1, F_2) , \quad (8)$$

where $P(F_1, F_2)$ and $Q(F_1, F_2)$ are the functions of F_1 and F_2 , and can be determined by the least-squares fit.

The QW model has been proposed to treat the exponential-tail state problem for structurally disordered materials by Chan, Louie, and Phillips.⁶ It is assumed in this treatment that a state of energy in the gap near the top of the valence band is due to potential fluctuations, which are modeled by QW's, and that the localized-tail

states in the gap of glassy semiconductors are produced by the potential fluctuations frozen in at T_g . As a consequence, they have found that the localized-tail states have approximately exponential behavior over a range of physical interest, and there exists a proportionality relationship between the width of the exponential-tail state (kT_0) and kT_g with a constant factor near 1.3, i.e.,

$$T_0 \simeq 1.3 T_g . \quad (9)$$

On the basis of this theoretical result, Ksendzov *et al.*⁵ experimentally established a direct relation between the Urbach-tail slope and the glass-transition temperature in some chalcogenide glasses.

The potential fluctuation frozen in at T_g assumed in the theoretical treatment is based on the fact that the large-scale atomic motions hardly take place below T_g .²² This assumption is reasonable for bulk glasses prepared by melt quenching. We note that structural properties of chalcogenide thin films deposited on substrates held at T_g by vacuum evaporation are similar to those obtained by quenching from the melt, because the annealing occurs simultaneously with the deposition process.²² Transient transport properties of the thin-film chalcogenides, which we examine here, are thereby similar to those of the melt-quenched glasses.^{20,23} Indeed, a relationship like Eq. (9) can be observed in *a*-As₂Se₃ and *a*-Se thin films.^{11,24} It is therefore reasonable that the above assumption is also valid for the thin-film samples.

In order to explain the experimentally obtained relation [Eq. (4)], we use some physical values appropriate for various Se-based glasses: $\nu = 10^{12}$ Hz, $\mu_0 = 10^{-2} \sim 10^0$ cm²/V s,^{11,24-26} and the experimental parameters $L = 1 \sim 100$ μm , $F_1 = 10^4$ V/cm, and $F_2 = 10^5$ V/cm.^{1,2,13,14,16-20} Substituting these parameters and Eq. (9) into Eq. (7), we obtain

$$E_0 = (1.2 \sim 2.0) \times 10^{-3} T_g . \quad (10)$$

This equation is in excellent agreement with Eq. (4).

The other important physical quantity which characterizes transient charge transport is the microscopic mobility, and hence we examine a relation between μ_0 and T_g as well. The μ_0 values have been obtained from the mobility at $T = T_0$. Figure 3 shows the dependence of the microscopic mobility on T_g in the Se-based chalcogenides. The μ_0 values are scattered in the range from 10^{-2} to 10^0 cm²/V s, which agrees well with the above-mentioned range, but seems to be independent of T_g . We consider that the microscopic mobilities independent of T_g are due to the fact that the top of the valence band is formed by nonbonding, lone-pair *p* orbitals at the Se atoms in the Se-based chalcogenides.²⁷

Finally, we would like to mention two important points deduced from Eqs. (5) and (8). First, the origin of the disagreement between the experimental β and the Poole-Frenkel coefficient can be explained; β is expressed as Eq. (8) and is not related to the dielectric constant in the case where the MT in an exponential-tail state plays a role. Second, the mechanism of the Meyer-Neldel correlation between the activation energy and the preexponential fac-

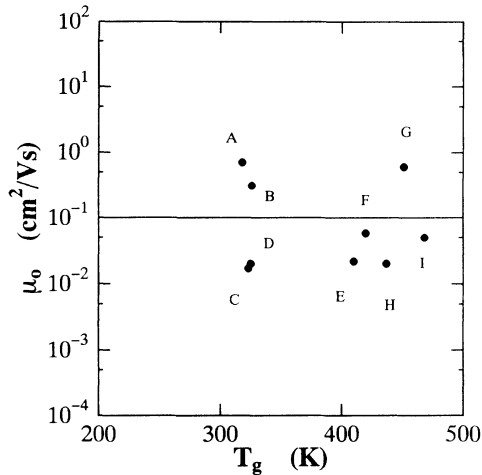


FIG. 3. Dependence of microscopic mobility, μ_0 , on the glass-transition temperature T_g for Se-based chalcogenides. Data for (A) *a*-Se (Ref. 13); (B) *a*-(5 at. % As):Se (Ref. 14); (C) *a*-(3.2 at. % Te):Se (Ref. 17); (D) *a*-(5 at. % Te):Se (Ref. 17); (E) *a*-(8 at. % Te):As₂Se₃; (F) *a*-(4 at. % Te):As₂Se₃; (G) *a*-GeSe₄ (Ref. 18); (H) *a*-AsSe (Ref. 19); and (I) *a*-As₂Se₃ (Ref. 20).

tor of the drift mobility can also be explained. Figure 4 shows the preexponential factor versus the activation energy obtained at various applied electric fields in *a*-As₂Se₃. A good correlation between these two quantities can be seen. The Meyer-Neldel rule can be observed in a great many activated processes, and states that if a process X obeys $X = X_0 \exp(-E/kT)$, the X_0 and E obey $X_0 = X_{00} \exp(aE)$, where X_{00} and a are constants. From the above two equations, we have

$$X = X_{00} \exp(aE) \exp(-E/kT). \quad (11)$$

Note that if we write $X = \mu_d$, $X_{00} = \mu_0/2$, and $a = 1/kT_0$, this equation is identical to Eq. (5), indicating that the transient charge transport due to the MT in an exponential-tail state exhibits the Meyer-Neldel relation. This interpretation is consistent with that reported by Jackson in hydrogenated amorphous silicon.²⁸

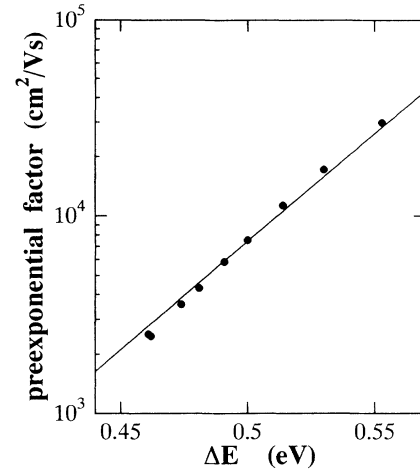


FIG. 4. The preexponential factor of the hole drift mobility vs the activation energy obtained at various electric fields in *a*-As₂Se₃. The solid line is the calculated line using Eq. (5) with the best-fitted physical parameters ($T_0 = 470$ K and $\mu_0 = 0.05$ cm²/Vs).

IV. CONCLUSIONS

We have investigated correlations between the transient transport properties and the glass-transition temperature in amorphous Se-based chalcogenides. A phenomenological relation has been found; the extrapolated zero-field drift-mobility activation energies vary as $1.2 \times 10^{-3} T_g$ in the Se-based chalcogenides. We show that the relation of the chalcogenides is successfully explained in terms of a combination of the MT and QW models, indicating that the transport of free carriers at the valence-band mobility edge in the materials is controlled by MT due to the exponential-tail state, whose width is solely determined by T_g . In addition, we elucidate the origin of the disagreement between the experimental β and the Poole-Frenkel coefficient, and of the Meyer-Neldel correlation between the activation energy and the preexponential factor of the drift mobility through the theoretical consideration.

¹R. C. Enck and G. Pfister, in *Photoconductivity and Related Phenomena*, edited by J. Mort and D. M. Pai (Elsevier, Amsterdam, 1976), p. 297.

²J. Mort and G. Pfister, in *Electronic Properties of Polymers*, edited by J. Mort and G. Pfister (Wiley, New York, 1982), p. 215.

³S. Sakka and J. D. Mackenzie, *J. Non-Cryst. Solids* **6**, 145 (1971).

⁴K. Tanaka, *J. Non-Cryst. Solids* **59/60**, 925 (1983).

⁵A. Ksendzov, F. H. Pollak, G. P. Espinosa, and J. C. Phillips, *Phys. Rev. B* **35**, 2740 (1987).

⁶C. T. Chan, S. G. Louie, and J. C. Phillips, *Phys. Rev. B* **35**, 2744 (1987).

⁷G. Pfister and H. Scher, *Phys. Rev. B* **15**, 2062 (1977).

⁸G. Pfister, *Phys. Rev. Lett.* **36**, 271 (1976).

⁹T. Tiedje and A. Rose, *Solid State Commun.* **37**, 49 (1980).

¹⁰J. Orenstein and M. Kastner, *Phys. Rev. Lett.* **46**, 1421 (1981).

¹¹J. Orenstein, M. A. Kastner, and V. Vaninov, *Philos. Mag. B* **46**, 23 (1982).

¹²D. Monroe, *Phys. Rev. Lett.* **54**, 146 (1985).

¹³S. O. Kasap and C. Juhász, *J. Phys. D* **18**, 703 (1985).

¹⁴C. Juhász and S. O. Kasap, *J. Phys. D* **18**, 721 (1985).

¹⁵M. Burman and J. Hirsch, *J. Non-Cryst. Solids* **35/36**, 987 (1980).

¹⁶H. Bäßler, G. Schönherr, M. Abkowitz, and D. M. Pai, *Phys. Rev. B* **26**, 3105 (1982).

¹⁷S. O. Kasap and C. Juhász, *J. Non-Cryst. Solids* **72**, 23 (1985).

¹⁸Gi Il Kim and J. Shirafuji, *Jpn. J. Appl. Phys.* **17**, 1789 (1978).

¹⁹F. D. Fisher, J. M. Marshall, and A. E. Owen, *Philos. Mag.* **33**, 261 (1976).

²⁰G. Pfister, *Philos. Mag.* **36**, 1147 (1977).

²¹Z. U. Borisova, *Glassy Semiconductors* (Plenum, New York,

- 1981).
- ²²S. R. Elliott, *Physics of Amorphous Materials* (Longman, Essex, 1990).
- ²³L. P. Kazakova, E. A. Lebedev, and E. A. Smorgonskaya, *Fiz. Tekh. Poluprovodn.* **16**, 2077 (1982) [*Sov. Phys. Semicond.* **16**, 1342 (1982)].
- ²⁴H. Naito, T. Iwai, M. Okuda, T. Matsushita, and A. Sugimura, *J. Non-Cryst. Solids* **114**, 112 (1989).
- ²⁵B. T. Kolomiets and T. F. Nazarova, *Fiz. Tverd. Tela (Leningrad)* **2**, 395 (1960) [*Sov. Phys. Solid State* **2**, 369 (1960)].
- ²⁶G. Juška, A. Matulionis, and J. Viščakas, *Phys. Status Solidi* **33**, 533 (1969).
- ²⁷M. Kastner, *Phys. Rev. Lett.* **28**, 355 (1972).
- ²⁸W. B. Jackson, *Phys. Rev. B* **38**, 3595 (1988).